Final Draft
of the original manuscript:

Dobron, P.; Bohlen, J.; Chmelik, F.; Lukac, P.; Letzig, D.; Kainer, K.U.:

Acoustic emission during stress relaxation of pure magnesium and AZ magnesium alloys

In: Materials Science and Engineering A (2006) Elsevier

DOI: 10.1016/j.msea.2005.12.111

ACOUSTIC EMISSION DURING STRESS RELAXATION OF PURE MAGNESIUM AND AZ MAGNESIUM ALLOYS

PATRIK DOBROŇ[1*], JAN BOHLEN[2], FRANTIŠEK CHMELÍK[1], PAVEL LUKÁČ[1], DIETMAR LETZIG[2], KARL ULRICH KAINER[2]

[1]Department of Metal Physics, Charles University, Ke Karlovu 5, CZ 121 16 Prague 2, Czech Republic

[2]GKSS-Forschungszentrum GmbH, Max-Planck-Str. 1, D-21502 Geesthacht, Germany

Abstract:

Acoustic emission (AE) was monitored and analysed during tensile tests of pure Mg and Mg alloys of AZ series in order to study the influence of the alloy composition on plastic deformation. The Kaiser effect was used to determine the stability of microstructure. During the tests at room temperature, repeated stress relaxations were performed. The solute – dislocation interaction in the alloys leads to ageing phenomenons, which are manifested as the post-relaxation effect and subsequent serrated flow (Portevin – Le Chatelier effect). The post-relaxation effect was sensitive to the alloy composition and to the strain, at which the stress relaxation was performed.

Key words: acoustic emission, stress relaxation, magnesium alloys, Kaiser effect

*corresponding author, e-mail: dobronp@karlov.mff.cuni.cz

Tel., fax: + 420 2 21911490

1. Introduction

Magnesium wrought alloys of the AZ family are of actual interest for the use as structural components due to the possibility to obtain even improved and more homogenous properties compared to cast components. Especially extrusion as a form giving technology offers the possibility to produce such profiles that are long and/or have a thin-walled structure [1-3]. The process parameters significantly influence the microstructural evolution e.g. in terms of the grain size and grain size distribution of the material and, consequently, influence the mechanical properties of the resulting profile [4].

Whereas the influence of solute atoms on the grain structure of extruded AZ alloys has already been reported in our previous paper [5], further attention must be given to the equally important solid solution strengthening in these alloys.

In principle, the solid solution strengthening is result of three interplaying modes of the solute – dislocation interaction: solid solution hardening, (quasi-) static ageing (SA) and dynamic strain ageing (DSA), respectively [6]. The effects of SA and DSA have already been observed in Mg alloys [7-9].

Acoustic emission (AE) stems from transient elastic waves which are generated within the material during deformation due to sudden localized and irreversible structure changes like dislocation glide and twinning, which are the main deformation mechanisms in Mg and its alloys due to their hexagonal crystal structure. Thus AE parameters can be used as a measure for the dynamic processes that play a role during plastic deformation of magnesium alloys [10]. Specifically, the so called Kaiser effect can be tested through repeated stress relaxations. The Kaiser effect is described as the absence of detectable AE at a fixed sensitivity level, until previously applied stress levels are exceeded [11]. The violation of the Kaiser effect indicates microstructure changes (as recovery or recrystallization) e.g. during unloading or stress relaxations.

The objective of the present paper is an AE study on the influence of solutes on the tensile deformation behavior of three AZ alloys fabricated by extrusion process. To reveal the effects of solid solution strengthening, pure Mg and the alloys were deformed at room temperature and at moderate strain rate and isochronal stress relaxations were applied.

2. Experimental procedure

The rod profiles of pure Mg in high purity quality and the alloys AZ31 (Mg + 2.9 wt.% Al + 0.98 wt.% Zn + 0.29 wt.% Mn), AZ61 (Mg + 6.5 wt.% Al + 0.99 wt.% Zn + 0.20 wt.% Mn) and AZ80 (Mg + 8.5 wt.% Al + 0.51 wt.% Zn + 0.31 wt.% Mn) [12,13] were used for this study. The profiles were produced by indirect extrusion and air-cooling. More detail on the set-up and the procedure may be found in [1,3,13-15]. After the extrusion, grain sizes of Mg and the alloys AZ31, AZ61 and AZ80 were of 15, 22, 12 and 13 μm, respectively. The microstructures of the alloys are reported in [5].

The specimens (diameter 6 mm, gauge length 36 mm, following DIN 50 125) were deformed in a universal testing machine Zwick® Z50 in tension at room temperature (RT) at a constant strain rate of 10^{-4} s^{-1}. During deformation the machine was stopped after each 2 % of strain and the specimen was allowed to relax for 300 s.

The computer controlled DAKEL-XEDO-3 AE system was used to monitor AE on the basis of two-threshold-level detection, which yields a comprehensive set of AE parameters involving count rates $\dot{N}_{C1}$ and $\dot{N}_{C2}$ (count number per second [11]) at two threshold levels (giving total AE count and burst AE count by proper setting – see below). The burst AE occurs mainly as a consequence of an instable fashion of plastic deformation or degradation of materials. A miniaturized MST8S piezoelectric transducer (diameter 3 mm, almost point AE detection, a flat response in a frequency band from 100 to 600 kHz, sensitivity 55 dB ref. 1 V_{ef}) was attached on the specimen surface with the help of silicon grease and a spring. The total gain was 90 dB. The AE signal sampling rate was 4 MHz, the threshold voltages for the total AE count N_{C1} and for the burst AE count N_{C2} were 730 and 1450 mV, respectively. The full scale of the A/D convertor was ± 2.4 V.

3. Experimental results

The engineering stress – strain curves at RT with and without stress relaxations for pure Mg and the AZ alloys are depicted in Fig. 1. By comparison to pure Mg, the alloys in both test series show a hardening effect with increasing amount of alloying elements. Moreover, a pronounced post-relaxation effect, manifested by a small yield point (a stress increment after reloading indicating ageing during relaxation) followed by a serrated flow curve (indicating the Portevin – Le Chatelier effect, i.e. DSA), is found after each stress relaxation in the AZ alloys. On contrary, the stress – strain curves for pure Mg in the both testing modes and those without stress relaxation of alloys do not show any visible irregularities.

As can be seen from Fig. 2, the post – relaxation effect is stronger with increasing amount of foreign atoms and the stress increment after reloading shows also a dependence on strain. This dependence is a monotonically decreasing function in case of the AZ 31 alloy, whereas it exhibits a maximum at a strain of 10% in the other alloys.

The Figs. 3-6 show the correlation between the engineering stress *vs.* time curves with stress relaxations and the AE count rates. As in tensile tests without stress relaxation [5], the AE count rates show a distinct peak at the beginning of plastic deformation followed by a subsequent decrease of the AE activity. The strongest AE activity is observed in the AZ 31 alloy. Detailed pictures (Figs. 3b – 6b) show a complex behavior of AE due to stress relaxation and the post-relaxation effect. In pure Mg (Fig. 3b), once a relaxation started, the AE activity drops rapidly and re-appears only, when the sample becomes reloaded. Similar behavior is observed also in the AZ 31 alloy (Fig. 4b), but the AE signal remains significant during the whole relaxation. Such behavior is referred to the violation of the Kaiser effect [10, 16]. The AE activity during relaxation of the AZ 61 and the AZ 80 alloys (Fig. 5b, 6b) is very low and a stronger AE re-appears only after reloading at a stress level, where the sample has previously been let to relax, i.e. these alloys obey the Kaiser effect. The small yield point after the relaxation exhibits always a pronounced AE burst.

4. Discussion

In both testing regimes (tensile tests with and without relaxations), the AZ alloys show a strong hardening effect by comparison to pure Mg. This effect is due to solid solution hardening and precipitation hardening by the alloying elements. In addition, the AZ alloys exhibit also a post-relaxation effect consisting of a small yield point and subsequent Portevin – Le Chatelier (PLC) effect (DSA). The efficiency of ageing is characterized by the dependencies of the stress increments after reloading on strain (cf. Fig. 2). Whereas the strain dependence of $\Delta\sigma$ for the AZ 31 alloy is monotonically decreasing, the dependencies for the AZ 61 and AZ 80 alloys exhibit a pronounced peak at medium strain of 10%. This behavior can be explained if we assume that the number of solute atoms available for locking dislocations is constant but the number of dislocations increases steadily during the test. In the AZ 31 alloy, the solute locking is most effective at the beginning of the test, in the other alloys containing more Al the locking effect is much larger and it reaches a maximum after some strain hardening. A comprehensive analysis and discussion of this behavior may be found in [9].

The behavior of pure Mg and AZ alloys may easily be correlated with the AE response as shown in Figs. 3 – 6. The AE peak at the onset of plastic deformation and the subsequent decrease of the AE activity define 'master' count rates *vs.* time dependencies, whose shape remains unchanged if the stress relaxations are applied. It indicates that the main AE source mechanisms (twinning and dislocation glide) are not influenced by the stress relaxations. The characteristic first peak, related to the macroscopic yield point is usually explained by a massive dislocation multiplication and twinning (if present), which are excellent sources of AE. The following decrease of the AE count rates may be ascribed to the increasing density of forest dislocations which reduces the flight distance and the free length of moving dislocations [10] as well as exhausting of twinning activity.

The correlation between the AE data and the plastic behavior during the relaxation and after that needs a special attention. The violation of the Kaiser effect is seen by pure Mg and by the AZ 31 alloy. By pure Mg, AE drops rapidly after the relaxation onset and it re-appear only after reloading. Such behavior may be explained by an unstable microstructure during relaxation, e.g. recovery due to climb of dislocations, which can lead to re-opening of already closed dislocation sources. For the AZ 31 alloy, only a small decrease of the AE activity is observed, once the relaxation started. This may indicate that plastic deformation continues by collective dislocation movement and very probably through twinning during the stress relaxation. Consequently, the effect of solute locking due to stress relaxation seems to be negligible in this case.

On the contrary, the AZ 61 and the AZ 80 alloys obey the Kaiser effect, which shows that the solute locking is efficient enough to stabilize the microstructure during the relaxation through diffusion of alloying elements to dislocations.

The pronounced AE peak corresponding to the small yield point after the relaxation (missing by pure Mg) may be explained, in agreement with [8-10], by dislocation breakaway from solute atmospheres after the reloading.

5. Conclusions

The solute – dislocation interaction in the AZ alloys fabricated by indirect extrusion leads to considerable solute hardening and the post-relaxation effect consisting of small yield point and dynamic strain ageing. The post-relaxation effect increases with increasing amount of alloying elements and it is strain dependent. The acoustic emission results show that performing stress relaxations does not change the main deformation mechanisms, i.e. twinning and collective dislocation motion. In the AZ 61 and the AZ 80 alloys, the solute locking contributes to the stabilization of the alloy microstructure, which could be of application interests.

Acknowledgements

This work was supported by the Czech Grant Agency under grant 205/03/0071. It is also a part of the Research Plan MSM 0021620834 that is financed by the Ministry of Education, Youth and Sports of the Czech Republic.

REFERENCES

[1] W.H. Sillekens, J.A.F.M. Schade van Westrum, A.J. den Bakker, P.J. Vet, Materials Science Forum 426-432 (2003) 629-636.

[2] F. Lass, A. Mertz, E. Hombergsmeier, H. Lanzerath, P. Baumgart, P. Cordini, in: K.U. Kainer (Ed.), Proceedings of the 6th International Conference and Exhibition on Magnesium Alloys and their Applications 2003, Wiley-VCH Weinhaim (2004) 1026–1033.

[3] K.B. Müller, in: H.I. Kaplan (Ed.), Magnesium Technology 2002, TMS, 2002 187-192.

[4] K.U. Kainer, E. Doege, S. Janssen, T. Ebert, in: K.U. Kainer (Ed.), Magnesium Alloys and their Applications, Wiley-VCH Weinhaim (2000) 596–601.

[5] J. Bohlen, F. Chmelík, P. Dobron, D. Letzig, P. Lukác, K.U. Kainer: J. Alloys Compd., 378 (2004) 214-219.

[6] P. Haasen, Physical Metallurgy, 3rd enl. and rev. ed., Cambridge University Press, Cambridge, 1996, pp.353-380.

[7] Z. Trojanová, P. Lukác, P. Gábor, Z. Drozd, K. Máthis, Kovove Mater. 39 (2001) 368-378.

[8] Z. Trojanová, P. Lukác, Kovove Mater. 43 (2005) 73-80.

[9] Z. Trojanová, P. Lukác, K. Milicka, Z. Száraz, Mater. Sci. Eng. A 387-389 (2004) 80-83.

[10] C.R. Heiple, S.H. Carpenter., J. Acoustic Emission 6 (1987) 177-204.

[11] Standard Practice for Acoustic Emission Examination of Fiberglass Reinforced Plastic Resin, ASTM E 1067-85. Tank/Vessels, May 31, 1985.

[12] M.M. Avedesian, H. Baker (Eds.), ASM Specialty Handbook: Magnesium and

Magnesium Alloys, ASM International, 1999, pp. 258-261.

[13] J. Swiostek, J. Bohlen, D. Letzig, K.U. Kainer, in: K.U. Kainer (ed.) Proceedings of the 6th International Conference and Exhibition on Magnesium Alloys and their Applications 2003, Wiley-VCH Weinhaim (2004) 278-284.

[14] W.H. Sillekens, J. Bohlen, in: K.U. Kainer (Ed.) Proceedings of the 6th International Conference and Exhibition on Magnesium Alloys and their Applications 2003, Wiley-VCH Weinheim (2004) 1046-1051.

[15] M. Bauser, G. Sauer, K. Siegert, Strangpressen, Aluminium Verlag Düsseldorf, 2001, pp. 143-170.

[16] T.T. Lamark, F. Chmelík, Y. Estrin, P. Lukác, J. Alloys Compd. 378 (2004) 202-206.

Figure Captions

Fig. 1: The engineering stress – strain curves with (continuous line) and without (dotted line) stress relaxations for pure Mg and the AZ alloys.

Fig. 2: Strain dependence of the stress increment after reloading for the AZ alloys.

Fig. 3: (a) - the correlation between the engineering stress *vs.* time curve with stress relaxations and the AE count rates at two threshold levels for pure Mg, (b) – detail of the relaxation at 4% of strain.

Fig. 4: (a) - the correlation between the engineering stress *vs.* time curve with stress relaxations and the AE count rates at two threshold levels for the AZ 31 alloy, (b) – detail of the relaxation at 4% of strain.

Fig. 5: (a) - the correlation between the engineering stress *vs.* time curve with stress relaxations and the AE count rates at two threshold levels for the AZ 61 alloy, (b) – detail of the relaxation at 4% of strain.

Fig. 6: (a) - the correlation between the engineering stress *vs.* time curve with stress relaxations and the AE count rates at two threshold levels for the AZ 80 alloy, (b) – detail of the relaxation at 4% of strain.

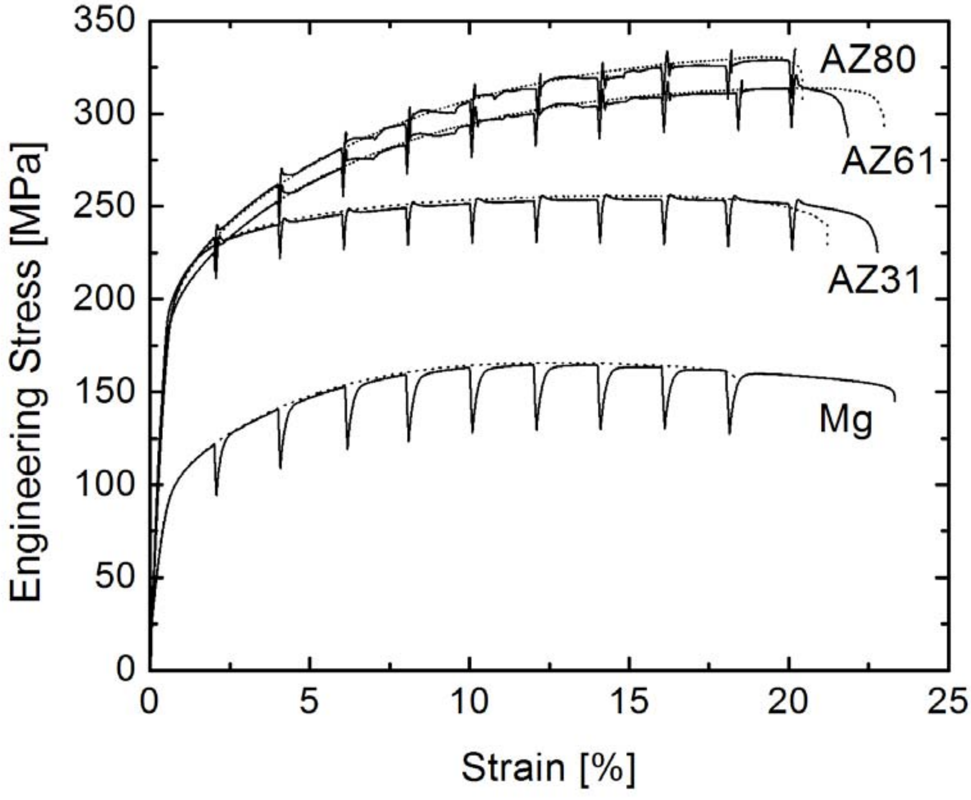

AZ80
AZ61
AZ31
Mg
Engineering Stress [MPa]
Strain [%]

Fig. 1.

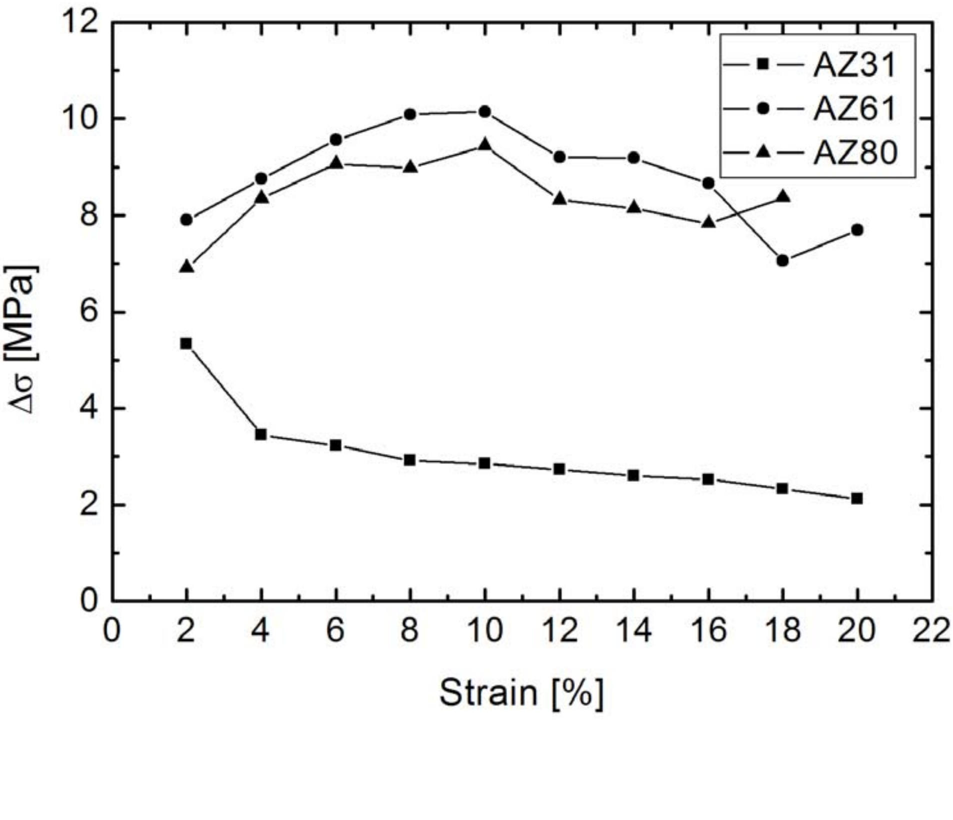

AZ31
AZ61
AZ80
Δσ [MPa]
Strain [%]

Fig. 2.

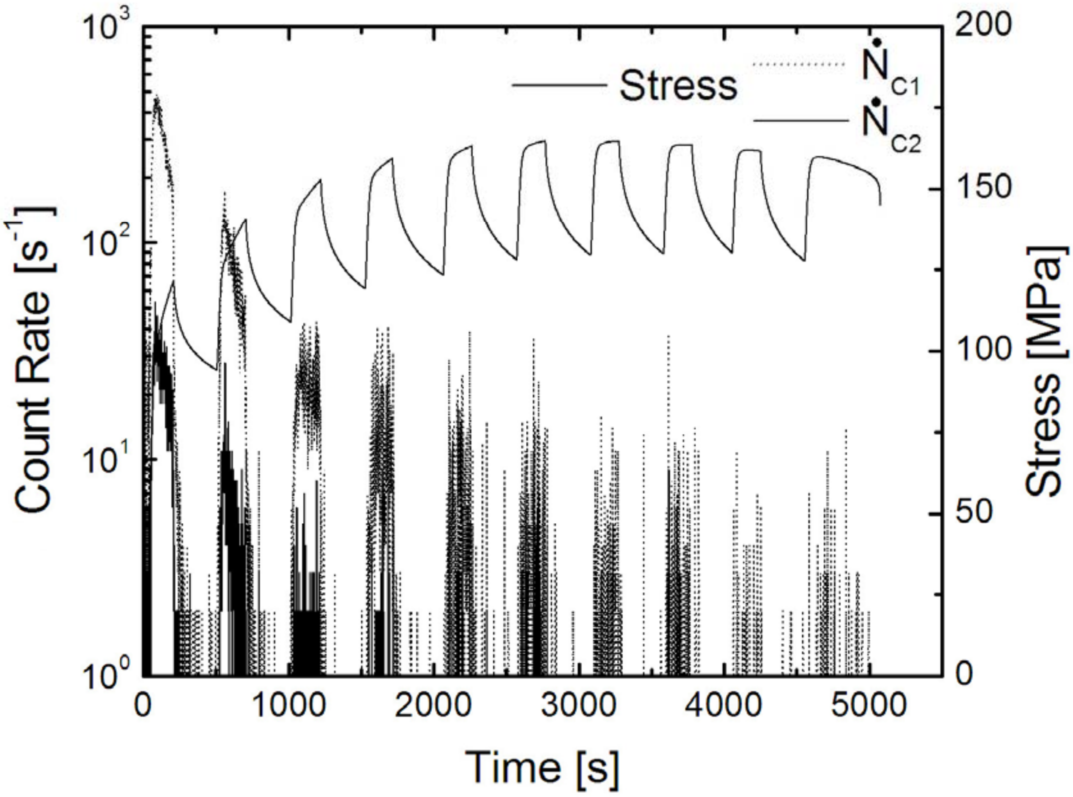

Stress
$\dot{N}_{C1}$
$\dot{N}_{C2}$
Count Rate [s^{-1}]
Stress [MPa]
Time [s]

Fig. 3a.

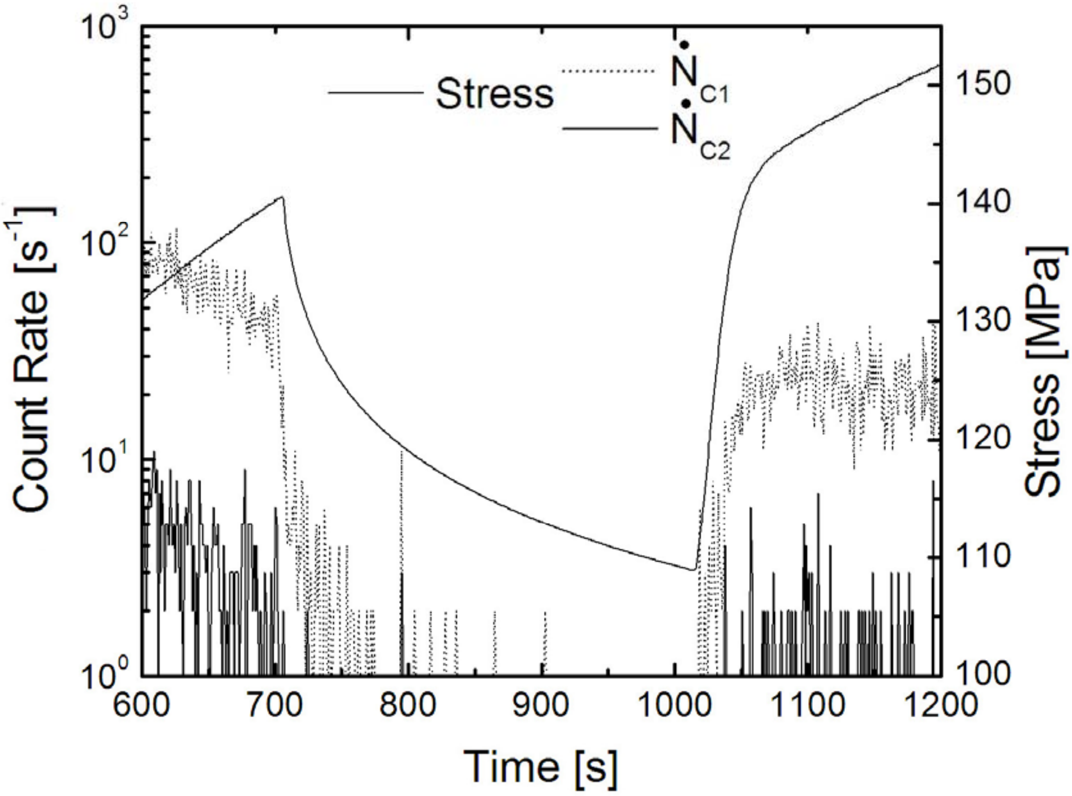

Stress
$\dot{N}_{C1}$
$\dot{N}_{C2}$
Count Rate [s^{-1}]
Stress [MPa]
Time [s]

Fig. 3b.

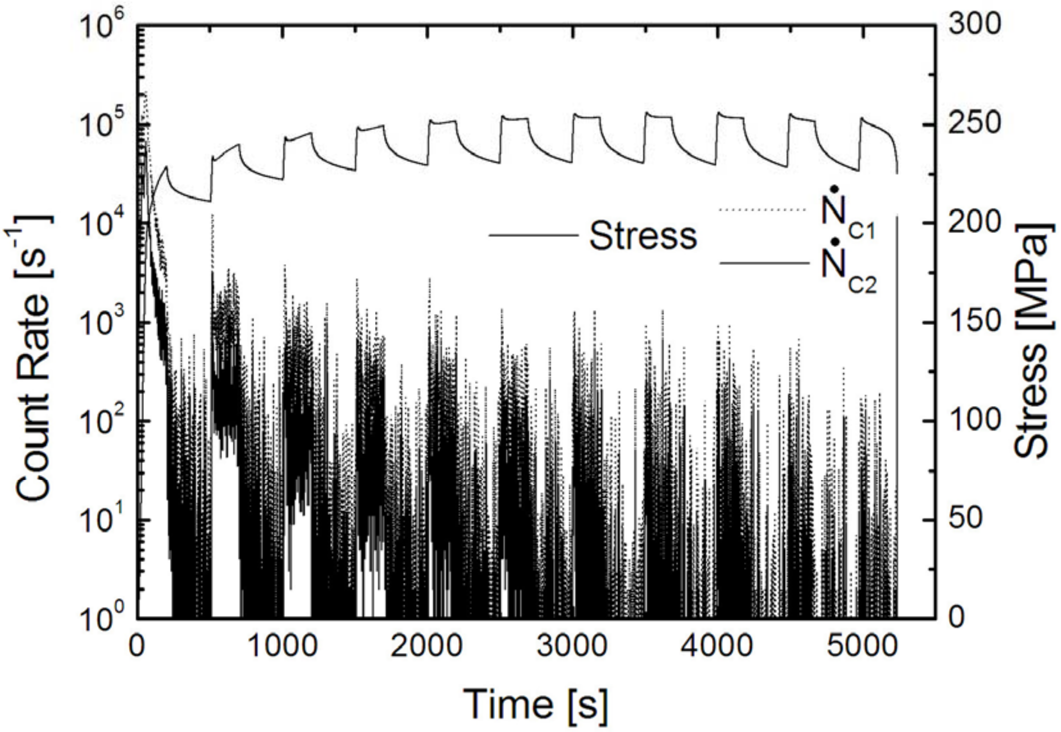

Count Rate [s-1]
Stress [MPa]
Time [s]
Stress
$\dot{N}_{C1}$
$\dot{N}_{C2}$

Fig. 4a.

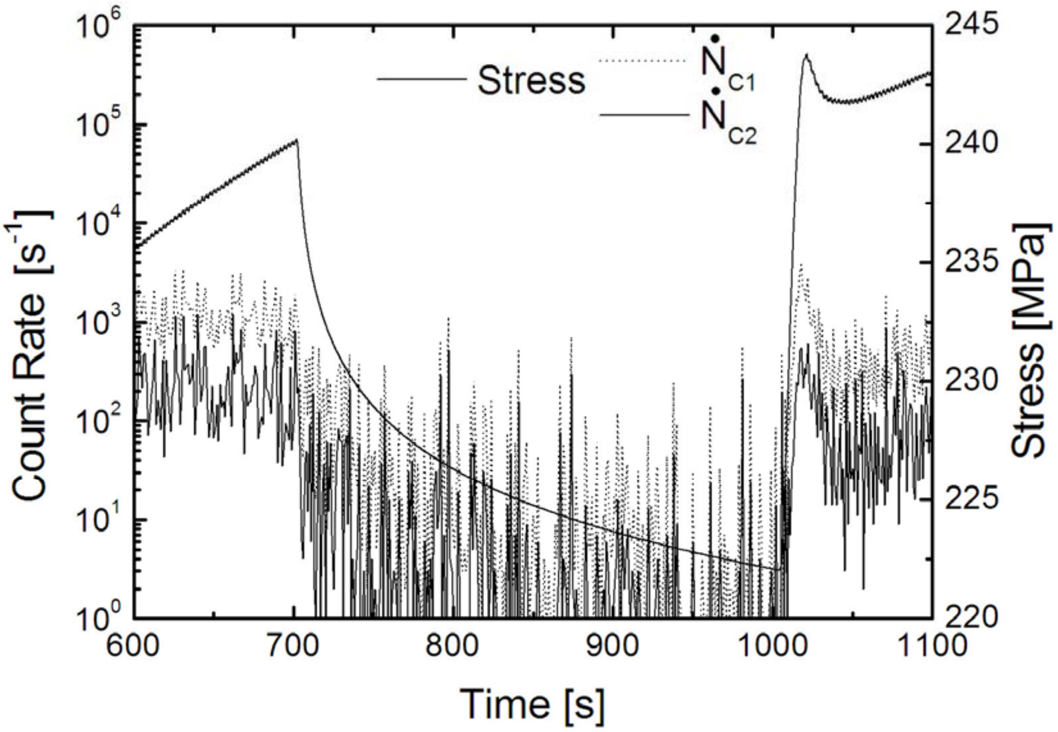

Count Rate [s-1]
Stress [MPa]
Time [s]
Stress
$\dot{N}_{C1}$
$\dot{N}_{C2}$

Fig. 4b.

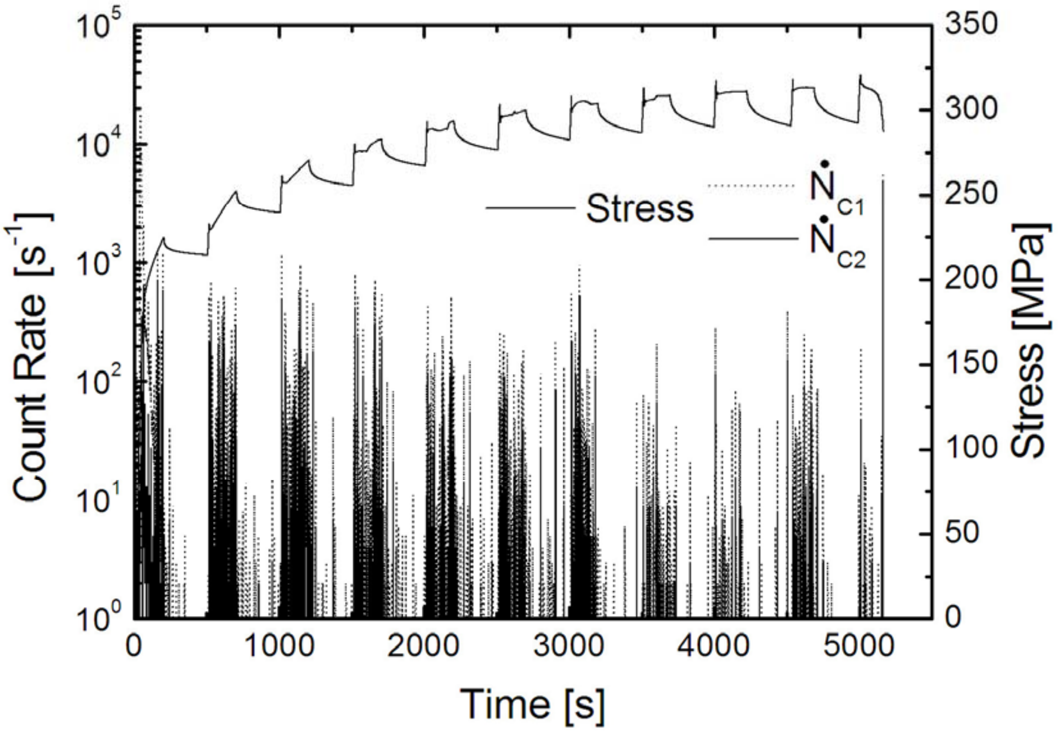

Count Rate [s-1]
Stress [MPa]
Time [s]
Stress
NC1
NC2

Fig. 5a.

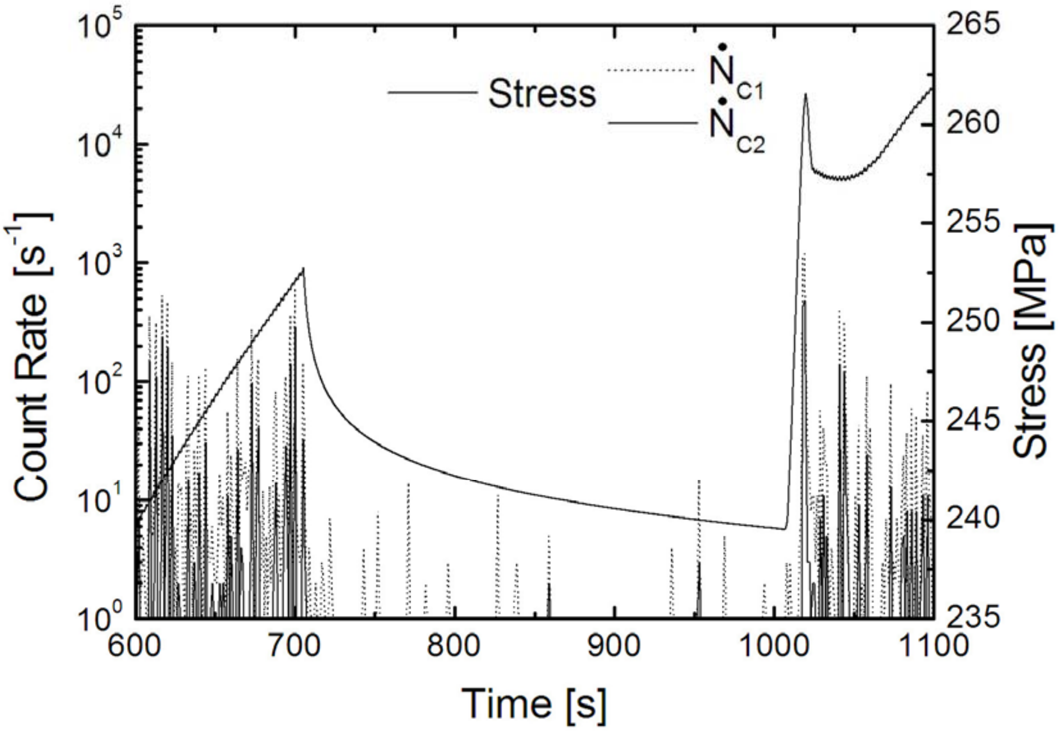

Count Rate [s-1]
Stress [MPa]
Time [s]
Stress
NC1
NC2

Fig. 5b.

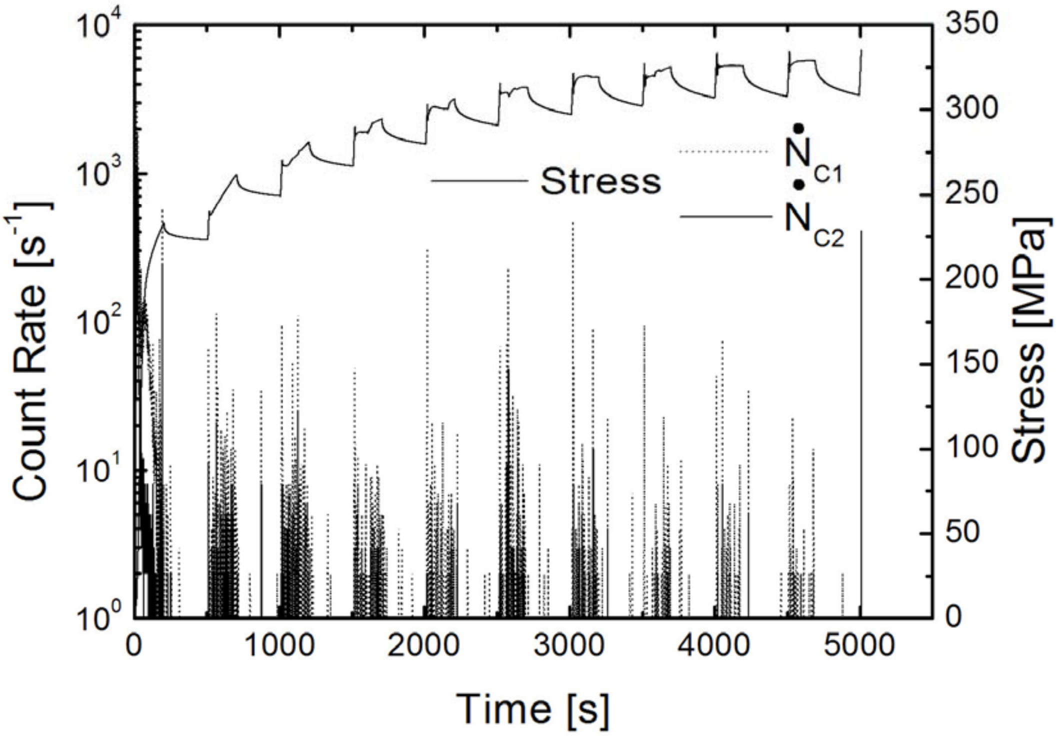
Stress
$\dot{N}_{C1}$
$\dot{N}_{C2}$
Count Rate [s^{-1}]
Stress [MPa]
Time [s]

Fig. 6a.

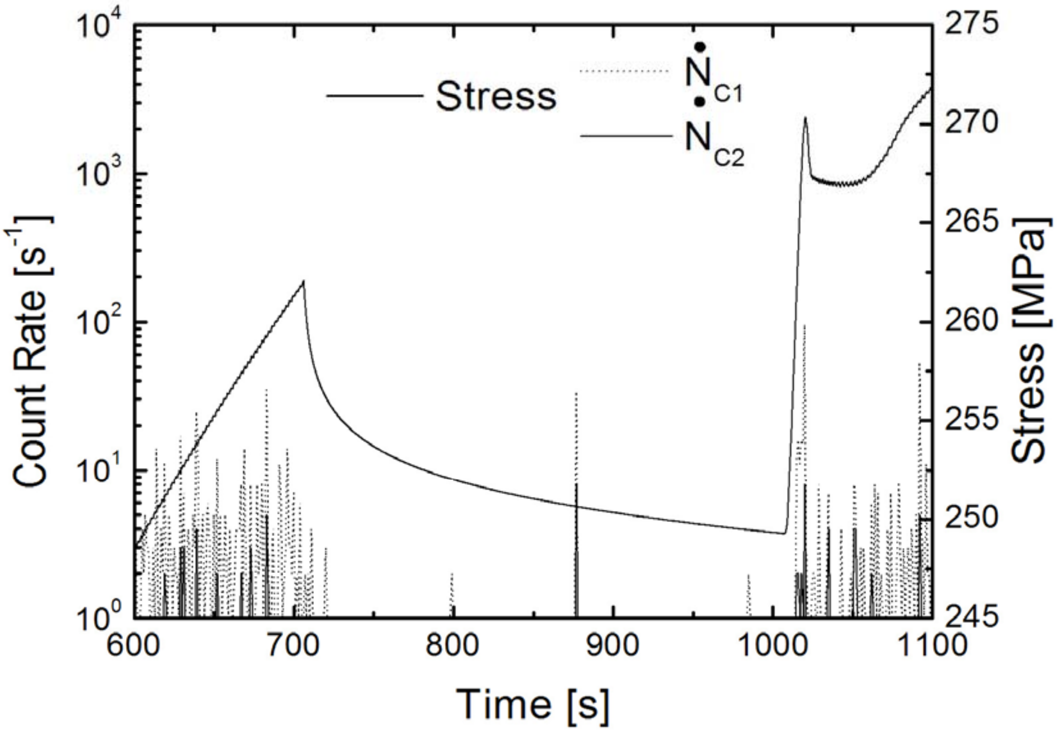
Stress
$\dot{N}_{C1}$
$\dot{N}_{C2}$
Count Rate [s^{-1}]
Stress [MPa]
Time [s]

Fig. 6b.